JOURNAL OF PROPULSION AND POWER
Vol. 16, No. 6, November–December 2000

Impingement Heating and Ignition of Condensed-Phase Energetic Materials

Mohammad K. Alkam*
Jordan University of Science and Technology, Irbid-Jordan
and
P. Barry Butler†
University of Iowa, Iowa City, Iowa 52242

A mathematical model is developed to simulate ignition of condensed-phase energetic materials by impingement of a hot gas jet. The hydrodynamics of the flow are considered to be steady state, while thermal transients take place with a step-temperature change at the jet upstream boundary condition. Condensed-phase chemical reactions are included in the model to account for the thermochemical changes within the energetic material because of heat addition at the exposed surface. The numerical method of lines is used to solve the governing equations in the gas and condensed phases. The results show the effects of several thermophysical properties on the ignition process including the hydrodynamic characteristics of the flow, the gas-temperature at the jet exit, the physical properties of the solid materials and the impinging gases, and the chemical kinetics of the energetic material. The current investigation also provides a discussion of the validity of some common assumptions appearing in the literature including semi-infinite solid geometry, one-dimensional modeling, steady-state treatment of the gas region, and the inert-heating approach.

Nomenclature

A_j = preexponential factor of the jth reaction step
Cp = specific heat, J/kg-K
Cp_s^* = effective specific heat defined in Eq. (3), J/kg-K
E_j = activation energy of the jth reaction step, J/kmol
e = emissivity
G = hydrodynamic quantity defined by Eq. (17), $(G = V_o/\nu r_o)$, 1/m^2
H = enthalpy, J
h = thickness of the solid disk, m
I = number of species
J = number of chemical reactions
k_j = rate constant of the jth reaction step, 1/s
l = thickness of the boundary layer, m
$\mathcal{L}$ = latent heat, J/kg
M_i = chemical symbol of the ith species
N_i = nondimensional progress variable of the ith species
Q_{ext} = total heat absorbed before ignition, J
q_j = heat of reaction of the jth reaction step, J/kg
q''_{rad} = net radiant heat flux absorbed at the solid surface, W/m^2
q''_s = heat flux at the stagnation point, W/m^2
q''_{ss} = steady-state heat flux at the stagnation point, W/m^2
r = radial coordinate, m
r_j = reaction rate of the jth reaction step, 1/s
r_o = jet radius, m
T = temperature, K
T_m = melting temperature of the solid material, K
T_o = temperature of the gases at the jet exit, K
T_{st} = stagnation point temperature, K
t = time, s
t_{ig} = ignition delay, s
u = axial velocity, m/s
V_o = velocity of the gases at the jet exit, m/s
v = radial velocity, m/s
z = axial coordinate, m
β_j = preexponential factor for the jth reaction step
Δt = time step, s
δ^* = delta form function
λ = thermal conductivity, W/m-K
μ_{ij} = elements of the concentration exponent matrix
ν = kinematic viscosity, m^2/s
ν' = stoichiometric coefficient of the reactants, kmol
ν'' = stoichiometric coefficients of the products, kmol
ν_{ij} = elements of the progress variable matrix
ρ = mixture density, kg/m^3
ρ_κ = density of the kth species, kg/m^3
σ = Stefan–Boltzmann constant, W/m^2-K^4

Subscripts

a = ambient
g = gas
i = species number i
j = reaction number j
o = jet exit
rad = radiation
s = solid phase
ss = steady state
$+$ = gas side of gas-solid interface
$-$ = solid side of gas-solid interface

Introduction

THIS study treats heating and subsequent ignition of condensed-phase energetic materials by impingement of a hot gas normal to the material's surface. The model is applied to several conventional energetic materials including tetranitro-tetrazacyclooctane (HMX), trinitro-triazacyclohexane (RDX), trinitrotoluene (TNT), and nitrocellulose (NC). Previously, Hobbs et al.[1] have investigated the ignition of several materials under constant heat flux and constant temperature boundary conditions. Their work showed that prior to ignition the portion of energetic material that gasifies is relatively small (<1% by mass). This observation, which combined the high speed typically associated with the hot gas, suggests that during impingement-ignition the dominant preignition reactions are the condensed-phase, sub-surface reactions. The solid-phase ignition

Received 18 September 1998; revision received 18 June 1999; accepted for publication 19 July 1999.

*Assistant Professor, Department of Mechanical Engineering, P.O. Box 3030-22110; mkalkam@mailcity.com.

†Professor, Department of Mechanical Engineering. Associate Fellow AIAA.

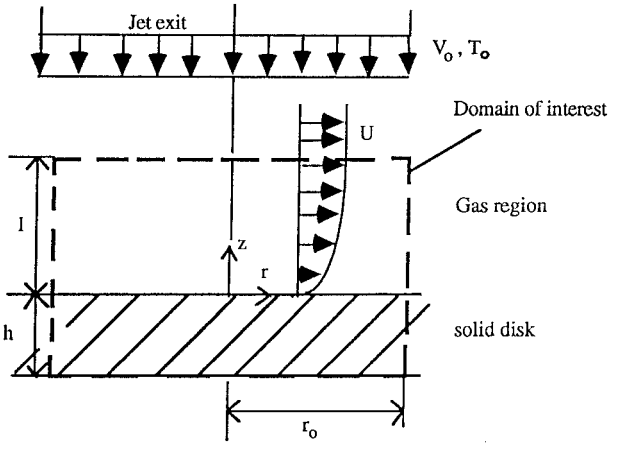

Fig. 1 Schematic diagram of system under consideration showing the coordinate system and the domain of interest.

theory adapted herein assumes surface and gas-phase reaction are negligible and focuses on the coupling of heat transfer to the condensed phase with condensed-phase chemistry.

Numerous articles have been published in the area of solid-propellant ignition. The literature covers a wide variety of operating conditions, several types of energetic materials with different chemical and physical characteristics, various kinds of external heat sources, and a wide range of rates of heat addition and different geometries. Kulkarni et al.[2] have presented a thorough review of the various ignition criteria adopted by previous researchers. Previous researchers who adopted solid-phase ignition theory include Kovalskii et al.,[3] Baer and Ryan,[4,5] Anderson,[6] Thompson and Suh,[7] Bradley,[8] and several significant contributions by Williams and coworkers.[9–13]

Figure 1 shows a schematic diagram of the physical system of interest. An axisymmetric, hot gas jet at temperature T_o and with a freestream velocity V_o impinges on the centerline of a solid disk of energetic material located at $z = 0$. The energetic material is initially at ambient temperature. The domain of interest includes the stagnation region within the gas flowfield and the solid material over a radius range of r_o and a thickness h. In Fig. 1 the domain of solution is bounded by the dashed line. The stagnation region under consideration is characterized by what is commonly referred to as the boundary-layer region. The width of the boundary-layer is approximately equal to the jet radius,[14] and the boundary layer-thickness l depends on the flow hydrodynamics. The hydrodynamics of the system are assumed to be steady state. In other words, the time needed to reach a steady-state velocity distribution is assumed to be much less than the ignition delay time. In view of this assumption, combined with the assumption of no gasification of the energetic material before onset of ignition, the well-known stagnation point Heimenz-flow[15] analysis is used to describe the velocity field in the gas region of the system under consideration.

The chemical reaction mechanism employed in a similar study by Hobbs et al.[1] has been adopted for these materials. The reaction mechanisms included in the model are multistep, Arrhenius-type chemical reactions. The solid-phase ignition theory used here states that the dominant reactions are those within the solid. Hence, gas-phase and heterogeneous reactions are neglected. This assumption can be justified for the following reasons: 1) the high speed of the impinging gases, 2) the small diameter of the jet, and 3) the inert nature of the impinging gases prevents heterogeneous reactions between the solid and the ambient gases.

Mathematical Model

The energy equations for fluid and solid phases have been cast in terms of temperature assuming negligible viscous dissipation and temperature-dependent physical properties. The resulting boundary-layer energy equation for the fluid region is

$$\rho_g C p_g \left(\frac{\partial T}{\partial t} + u \frac{\partial T_g}{\partial z} + v \frac{\partial T_g}{\partial r} \right) = \frac{\partial}{\partial z} \left(\lambda_g \frac{\partial T_g}{\partial z} \right) \tag{1}$$

and the temperature field within the condensed-phase energetic material is described by the following equation for multicomponent reacting system:

$$\rho_s C p_s^* \frac{\partial T_s}{\partial t} = \frac{1}{r} \frac{\partial}{\partial r} \left(\lambda_s r \frac{\partial T_s}{\partial r} \right) + \frac{\partial}{\partial z} \left(\lambda_s \frac{\partial T_s}{\partial z} \right) + S_{\text{total}} \tag{2}$$

In Eq. (2), S_{total} is a source term accounting for condensed-phase chemical reactions. These reactions are simulated by a three-step reduced reaction mechanism. Because no material depletion or expansion is considered to take place, the density of the solid is assumed constant. For the energetic materials under consideration, values of the thermal conductivities and the specific heats as functions of temperature are taken from Ref. 1. It is well known that some condensed-phase energetic materials melt before ignition takes place, providing an energy sink for the applied heat flux. The latent heat of melting was considered in the analysis by using the effective capacitance model.[16] In Eq. (2) Cp_s^* is an effective specific heat defined as

$$Cp_s^* = \frac{\mathrm{d}H}{\mathrm{d}T} = Cp_s + l\delta^*(T - T_m, \Delta T) \tag{3}$$

where $\delta^*(T - T_m, \Delta T)$ is the delta form function that has a finite value in the interval $\Delta T = 2$ K around T_m and is zero outside this interval. Accounting for the latent heat in this manner is computationally efficient[17] because the two-phase region with a jump condition is reduced to a single phase with rapidly varying properties.

Initial and Boundary Conditions

The initial and boundary conditions simulate the instantaneous introduction of a hot fluid on the top surface of a solid disk of reactive energetic material. The gas/solid system is initially at the ambient temperature T_a, and the jet outlet is at T_o, where $T_o \gg T_a$. The solid disk lateral boundaries are treated as adiabatic, and the bottom boundary is isothermal. These imposed conditions, in addition to the symmetry of the temperature distribution at the jet centerline, and the continuity of both temperature and heat flux at the interface can be summarized as follows:

$$T_s(r, z, 0) = T_g(r, z, 0) = T_a \tag{4}$$

$$T_g(r, l, t) = T_o \tag{5}$$

$$\frac{\partial T_s}{\partial r}(0, z, t) = \frac{\partial T_g}{\partial r}(0, z, t) = 0 \tag{6}$$

$$\frac{\partial T_s}{\partial r}(r_o, z, t) = 0 \tag{7}$$

$$T_s(r, -h, t) = T_a \tag{8}$$

$$T_g(r, 0^+, t) = T_s(r, 0^-, t) \tag{9}$$

$$\lambda_g \frac{\partial T_g}{\partial z}(r, 0^+, t) + q''_{\text{rad}} = \lambda_s \frac{\partial T_s}{\partial z}(r, 0^-, t) \tag{10}$$

$$q''_{\text{rad}} = \sigma \left(a_g e_g T_o^4 - e_s T_s^4 \right) \tag{11}$$

Here, the solid is assumed to be a blackbody ($a_s = e_s = 1$), and the calculation of the gas total emissivity was taken from Smith et al.[18] for atmospheric pressure and an optical length of 0.02 m.

Chemical Species Rate Equations

For J reactions that involve I species, the reaction source term S_{total}, given in Eq. (2), is determined by the following expression:

$$S_{\text{total}} = \sum_{i=1}^{I} \sum_{j=1}^{J} q_j \rho_i r_{ij} \tag{12}$$

where the general reaction scheme is

$$\sum_{i=1}^{I} \nu'_{ij} M_i \rightarrow \sum_{i=1}^{I} \nu''_{ij} M_i \qquad j = 1, \ldots, J \tag{13}$$

For each of the J reaction steps, the reaction rate r_j is defined as

$$r_j = k_j(T) \prod_{i=1}^{I} N_i^{\mu_{ij}} \qquad j = 1, \ldots, J \tag{14}$$

The rates of change of species are given by

$$\frac{dN_i}{dt} = \sum_{j=1}^{J} \nu_{ij} r_j \qquad i = 1, \ldots, I \tag{15}$$

In Eq. (14) the specific reaction rate constant k_j are given in an Arrhenius form as

$$k_j(T) = T^{\beta_j} A_j \exp(-E_j / RT) \tag{16}$$

In the present investigation the reduced reaction mechanisms as well as the corresponding kinetic rate data for the energetic materials under consideration are taken from the experimental work by McGuire and Tarver.[19]

Numerical Methodology

As common in many transient combustion problems, several distinct timescales are present in the present system. These timescales include the diffusion, the convection, and the chemical reaction timescales. There is a wide variation between the three timescales present. This fact motivated the choice of the numerical method of lines,[20] which is known to be convenient for problems with several distinct timescales. Here, the spatial derivatives within the governing equations are discretized by an explicit, upwind finite difference scheme. Initially, the discretized governing equations along with the discretized initial and boundary conditions were applied to every node in the computational domain yielding a system of coupled, ordinary differential equations. The LSODE algorithm[21] was used to integrate numerically the resulting system of equations over a finite time step Δt yielding values of temperature and species concentrations. The magnitude of the time step was chosen by numerical experimentation to ensure numerical stability and to obtain a solution that is independent of the time step.[22] It was also assured the time step was small enough to capture the chemical changes within the system. In the present calculations a time step of $\Delta t = 0.01$ ms was used. The whole procedure was repeated to march the solution with time. A computer FORTRAN program (IGNITION2D) was constructed to carry out the numerical computations.

Results

The problem under consideration is characterized by a jet of hot gas impinging on the surface of a solid disk of reactive material. The present model was applied to five conventional energetic materials: HMX, RDX, TNT, 1,3,5-triamino-2,4,6-trinitropenzene (TATB), and NC. It is important to identify the important parameters that affect the heat flux at the gas-solid interface because it plays a major role in characterizing the ignition conditions. These parameters include the temperature of the impinging gas at the jet exit, the physical properties of both the impinging gases and the solid material, and the thickness of the boundary-layer region that acts as a thermal insulator on the top surface of the solid material. In stagnation flow configurations the boundary-layer thickness is a function of a quantity that combines the effects of the jet radius r_o, the kinematic viscosity of the gas ν, and the velocity of the gases at the jet exit V_o. This quantity is referred to as G and is defined as[15]

$$G = V_o / \nu r_o \tag{17}$$

Equation (17) shows that G has a dimension of m^{-2}. In the present investigation G is used as one of the independent variables in the presentation of results, where G characterizes the gas hydrodynamics. A high value of G implies a thinner boundary-layer region, and, consequently, a higher heat flux at the gas-solid interface, whereas low Gs indicate low values of surface heat flux. The dependence of the heat flux at the gas-solid interface on G is shown later.

To solve the governing equations, the input parameters are 1) the thickness of the solid disk h, 2) the radius of the jet r_o, 3) the temperature of the gases at the jet exit T_o, 4) the physical properties of the impinging gas and the solid material as functions of temperature, 5) the hydrodynamic characteristics of the impinging gases (the quantity G), 6) the chemical kinetic information including reaction steps, Arrhenius kinetic parameters, heats of reactions, species involved, and activation energies, and 7) specification of the initial and boundary conditions. In the present section the quantitative results of the present investigation are presented. Several test cases were presented corresponding to different operating conditions and different types of gases and solid materials. According to the notation used in this work, NC-Helium (He) refers to a test case where helium gas impinges against a solid disk of NC, also HMX-Air means that air is used as the impinging gas, and HMX is used as the solid energetic material. In the test cases presented in this section, the radius of the jet r_o was 1 cm, and the thickness of the solid disk h was 0.5 cm, unless stated otherwise.

All investigations appearing in the literature review section employed one-dimensional geometries. In the present work the intention is to check the validity of this common assumption and to introduce a general statement regarding whether a two-dimensional consideration is necessary. A two-dimensional code (IGNITION2D) was developed to simulate the system under consideration. As was shown in preceding discussions, the physical system of interest consists of the stagnation region of hot impinging gases and a solid disk of a reactive energetic material (see Fig. 1). Several investigations[14,23] showed that within the stagnation region the heat flux at the gas-solid interface does not vary in the radial direction. In other words, if the lateral boundary of the solid disk is kept insulated, the heat transfer within the system of interest will take place only in the axial direction. This eliminates the need for the two-dimensionality. However, if heat transfer is allowed to take place through the lateral boundary of the solid disk, the heat flux as well as the temperature of the system will have radial variations, and, hence, the question of two-dimensionality arises.

Through solving the energy equation for a solid propellant numerically, each node within the grid setup has a source term corresponding to the chemical reactions that take place at that particular location. These source terms are highly dependent on the local temperature, and, hence, numerical solutions of such problems are expected to be quite sensitive to the grid size. In the present work numerical experiments were performed to achieve a solution independent of the grid size. The study showed that a grid-independent solution can be achieved for 150 grid nodes. To ensure accuracy, 170 grid nodes were considered through all of the computations that appear in the present work.

To investigate the validity the one-dimensional analysis for the present system, two cases were studied. Both cases included the impingement of He with $G = 1.0 \times 10^8$ m^{-2} and $T_o = 2000$ K against a solid disk of NC. In the first case the two-dimensional code (IGNITION2D) was run to simulate the present system imposing an adiabatic lateral boundary condition on the solid disk. This analysis resembled the one-dimensional case because no radial heat transfer took place. In the second case radial heat flux was allowed to take place through an isothermal lateral boundary where the temperature of the solid disk at the outer radius r_o was kept at 298 K. The stagnation-point temperature histories of both cases are shown in Fig. 2. Figure 2 shows that the stagnation-point temperature increases gradually with time and then accelerates rapidly at the onset of ignition. The drastic increase in the stagnation-point temperature at the ignition point is commonly known as the thermal run away. Thermal run away is one of the most-used ignition criteria in the study of solid propellants and is considered as the ignition criterion in the present work. Figure 2 shows no noticeable difference in ignition delay between the two cases. Thus, the conclusion was made that the one-dimensional analysis could successfully reproduce the results of the two-dimensional analysis in regards to ignition characteristics. However, this statement may not be generalized for arbitrary operating conditions. In general, for problems including ignition of the solid energetic materials under consideration, if the radial heat transfer is much smaller than the axial heat transfer one may consider the one-dimensional analysis for simulating the ignition characteristics of these materials. For the sake of

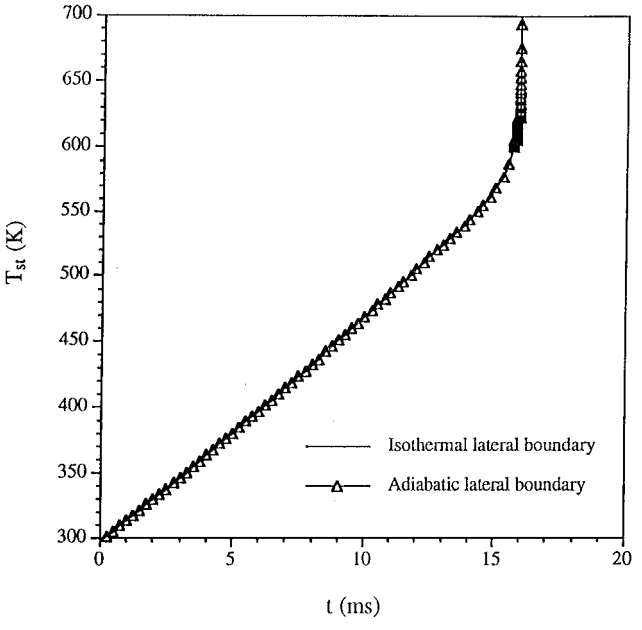

Fig. 2 Stagnation-point temperature history. Comparison with the cases of adiabatic lateral boundary and isothermal lateral boundary for NC-He, with $G = 1.0 \times 10^8$ m^{-2} and $T_o = 2000$ K.

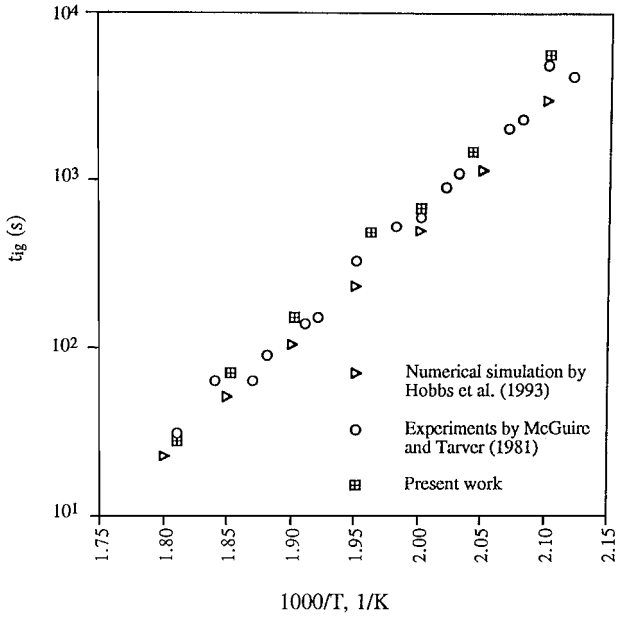

Fig. 3 Variation of the ignition delay t_{ig} with the temperature of an isothermal boundary of a spherical element of HMX with 1.27 diameter

the computational time and the storage requirement of the present analysis, the decision was made to use the one-dimensional version of the code (IGNITION1D).

To verify the credibility of the present analysis, the computer code IGNITION1D was used to solve the case of ignition of a spherical element of HMX subject to an isothermal boundary. The case was solved theoretically by Hobbs et al.[1] and examined experimentally by McGuire and Tarver.[19] Figure 3 shows the comparison between the present work and the previous results. The results are in agreement. Based on the configuration of these experiments, the comparison serves as a validation of the chemical kinetics, phase change, and thermal diffusivity components of the model.

Based on the fact that the solid energetic materials under consideration are poor heat conductors, several previous investigators treated the solid region as semi-infinite in length. Considering semi-infinite solid material implies that the bottom surface (the surface

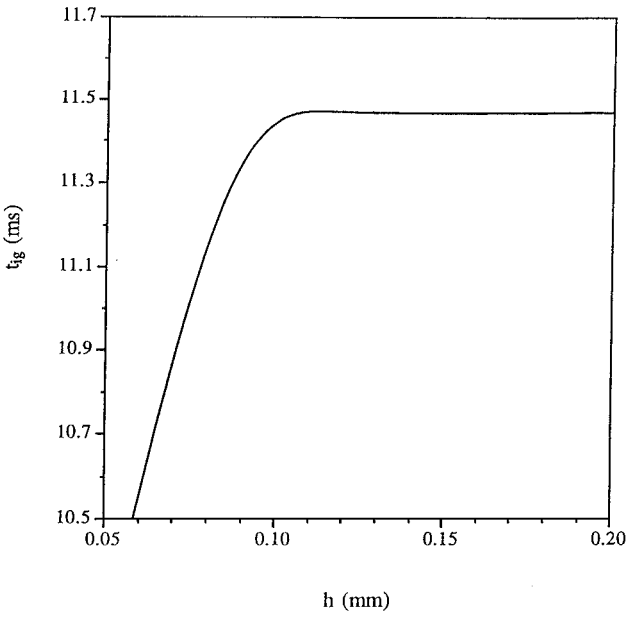

Fig. 4 Effect of the thickness of the solid region h on the ignition delay t_{ig} for NC-He, with $T_o = 2000$ K and $G = 1.0 \times 10^7$ m^{-2}.

unexposed to the gas jet) of the energetic material is not influenced by the thermal activities that take place near the top surface (the surface exposed to the gas jet) of the solid where ignition is expected to occur. Also, the assumption of semi-infinite solid geometry blinds the effect of the solid thickness on the ignition process. In the present work the solid material was assumed to have a finite thickness h. However, the feasibility of the assumption of semi-infinite geometry is investigated. For this purpose the effect of the thickness of the solid region on the ignition characteristics has been studied. The study showed that the ignition process is only affected by h in the limit of small values of h. For NC-He with $G = 1.0 \times 10^7$ m^{-2} and $T_o = 2000$ K, the effect of the solid thickness on the ignition delay is plotted in Fig. 4. The figure shows that for $h \leq 0.1$ mm t_{ig} increases monotonically with h until it reaches a constant value that is insensitive to the solid thickness. In other words the bottom of the solid does not have any impact on the thermal transients on top of the solid disk unless h is less that 0.1 mm. This is consistent with the fact that the energetic materials under consideration have relatively low thermal conductivities. Based on the study shown in Fig. 4, one can conclude that considering semi-infinite geometries for analyzing the ignition of the materials under consideration is a reasonable approach for high values of the thickness of the solid material.

The impact of the hydrodynamic characteristics of the impinging gases on the ignition process of the solid materials under consideration is of great importance to the present study. Figure 5 presents several curves that describe the stagnation-point temperature histories for HMX-He with $T_o = 2000$ K. Helium was chosen for the initial study because it acquires favorable thermal properties that make it a good medium for heat transfer. Each curve corresponds to a different value of the hydrodynamic parameter G defined earlier by Eq. (17). As shown in Fig. 5, G ranges from 2.0×10^7 to 1.0×10^8 m^{-2}. For each value of G, the stagnation-point temperature increases with time until it reaches the thermal run-away condition that resembles the onset of ignition. The time required for the stagnation-point temperature to reach the thermal run-away condition is referred to as the ignition delay. The observation can be made that the ignition delay decreases as G increases because of the increase of the heat flux at the gas-solid interface associated with the increase in G. One should notice that each temperature profile in Fig. 5 goes through two periods of constant temperature. The first is caused by the latent heat absorbed because of the phase change of the solid energetic material, and the second results from the endothermic reactions that simulate the fuel pyrolysis before the self-sustained ignition takes place.

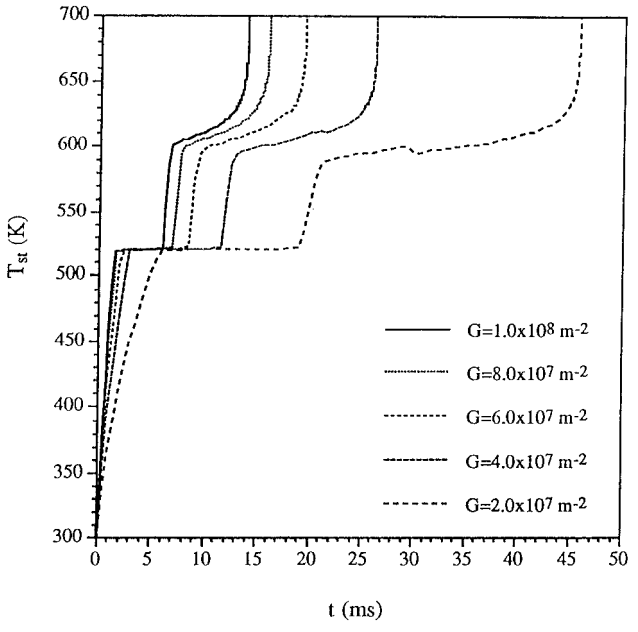

Fig. 5 Effect G on stagnation-point temperature history profiles for HMX-He with T_o = 2000 K. In each profile the first region of constant temperature is caused by the latent heat of phase change, and the second results from the endothermic reactions that simulate fuel pyrolysis before self-sustained ignition.

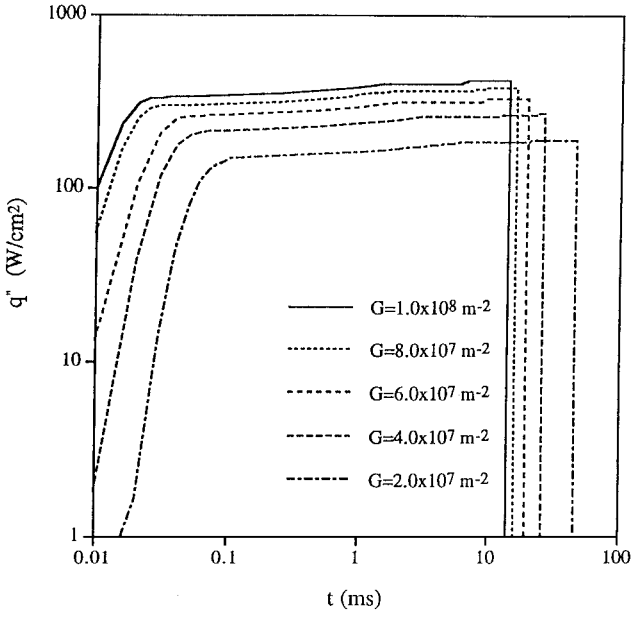

Fig. 6 Effect G on the heat-flux history at the stagnation point q_s for HMX-He with T_o = 2000 K.

The ignition characteristics of the solid energetic materials are determined by several factors including 1) the heat-flux history at the gas-solid interface, 2) the chemical kinetic characteristics of the chemical reactions within the solid material of interest, and 3) the physical properties of the solid materials, especially the thermal diffusivity. For a given solid material the major factor that affects the ignition characteristics of the specified system is the heat flux at the solid boundaries. To have a better feeling of the heat flux at the stagnation point in relation to G, the heat-flux q_s'' history was plotted in Fig. 6 for HMX-He with $T_o = 2000$ K. In Fig. 6 several cases were plotted corresponding to different values of G. It is quite clear that the value of the heat-flux increases as G increases, yet the figure shows that the heat-flux increases from zero, initially, up to a steady-state value q_{ss}'' before ignition takes place. Although the heat-

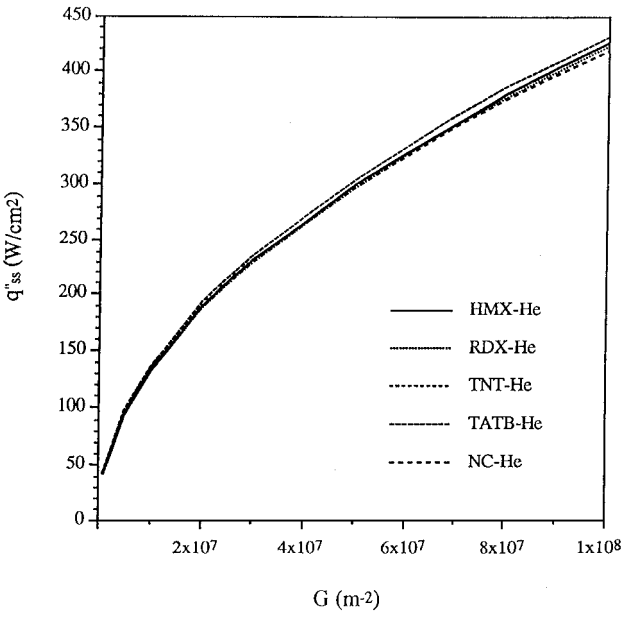

Fig. 7 Effect G on the steady-state heat flux at the stagnation point (q_{ss}'') for HMX-He, RDX-He, TNT-He, TATB-He, and NC-He with T_o = 2000 K.

flux appears to reach its steady-state value in a relatively short period of time, steady-state analysis cannot capture the thermal transients of the system accurately at early times and during the pyrolysis endothermic reactions, especially when G is less than 4.0×10^7 m^{-2}. For a helium jet with a temperature of 2000 K, the variation of the steady-state heat flux at the stagnation point q_{ss}'' with G is shown in Fig. 7. In the figure several curves are plotted corresponding to different gas-solid combinations, including HMX-He, RDX-He, TNT-He, TATB-He, and NC-He. From the basic heat-transfer principles the value of the steady-state heat flux is independent of the thermal diffusivity of the solid material in the absence of the heat source terms. Figure 7 shows that for low values of G ($G < 2.0 \times 10^7$ m^{-2}) the steady-state heat flux corresponding to the different solid materials is similar. This is because the heat flux reaches its steady-state value before the heat-source terms are activated. For higher values of G ($G > 2.0 \times 10^7$ m^{-2}), the heat-source terms contribute to the thermal transients of the system before the heat flux reaches its steady-state conditions, and, hence, some deviation among the curves begin to take place in Fig. 7.

For a given exit temperature the ignition delay decreases asymptotically as G increases. This behavior is shown in Fig. 8 for HMX-He, RDX-He, TNT-He, TATB-He, and NC-He with $T_o = 2000$ K. The figure shows that for the same operating conditions NC has the shortest ignition delay, whereas TATB takes the longest time to ignite. The comparison between the solid materials suggests that NC requires less energy addition than the other materials to acquire self-sustained ignition, whereas TATB requires more energy to ignite. This is consistent with the values of the activation energy for the reaction steps used to simulate the chemical changes within the solid materials investigated. The variation of the ignition delay with G is explained by the strong correlation between G and the heat flux at the gas-solid interface. Figure 9 is a graph of the ignition delay as a function of the steady-state heat flux at the stagnation point for HMX-He, RDX-He, TNT-He, TATB-He, and NC-He with $T_o = 2000$ K.

One other parameter of interest is the total amount of heat absorbed by the solid material before ignition takes place (Q_{ext}). This quantity is calculated by integrating the heat transfer over all of the solid boundaries. The value of Q_{ext} depends on several factors including 1) the activation energies of the individual reaction steps that simulate the chemical changes within the solid material, 2) the heat flux at the solid boundary, and 3) the rate of heat diffusion through the solid material. In Fig. 10 the variation of Q_{ext} with G

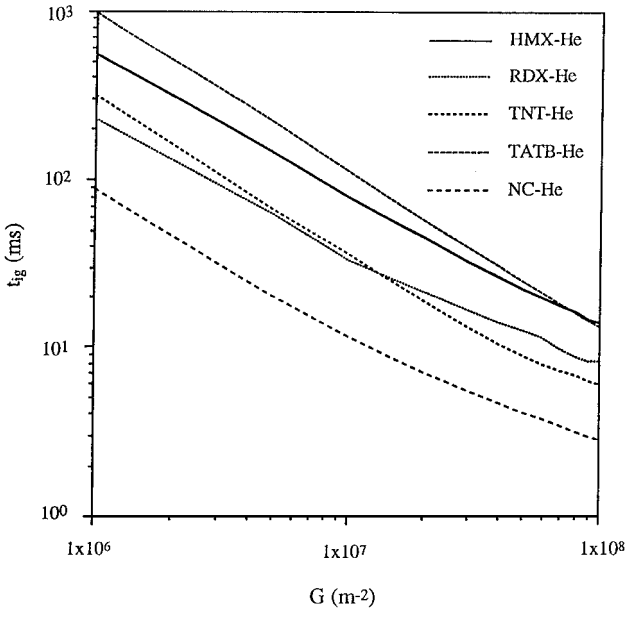

Fig. 8 Effect G on the ignition delay t_{ig} for HMX-He, RDX-He, TNT-He, TATB-He, and NC-He with T_o = 2000 K.

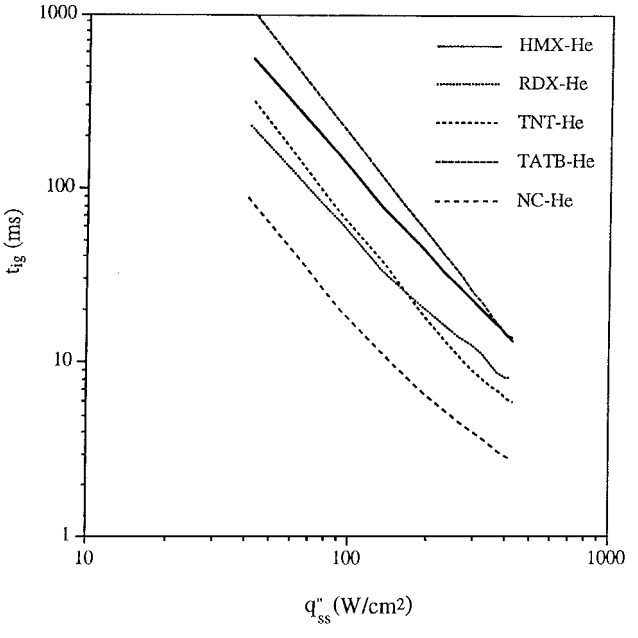

Fig. 9 Effect q''_{ss} on the ignition delay t_{ig} for HMX-He, RDX-He, TNT-He, TATB-He, and NC-He with T_o = 2000 K.

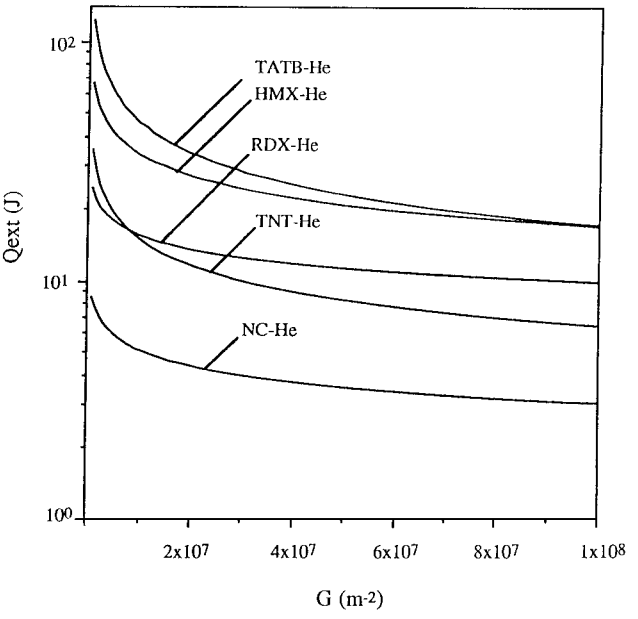

Fig. 10 Effect G on the amount of heat added to the solid material before ignition Q_{ext} for HMX-He, RDX-He, TNT-He, TATB-He, and NC-He with T_o = 2000 K.

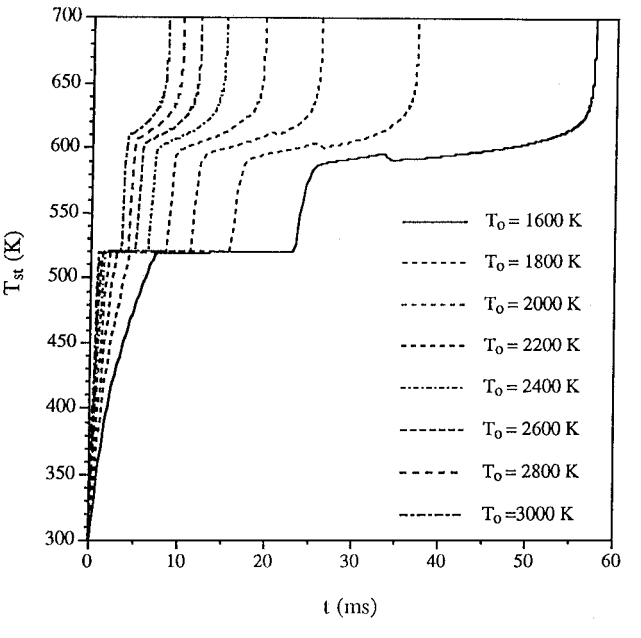

Fig. 11 Effect of T_o on stagnation-point temperature history profiles for HMX-He with $G = 4.0 \times 10^7$ m^{-2}.

is presented, and several cases are compared including HMX-He, RDX-He, TNT-He, TATB-He, and NC-He. The gas temperature at the jet exit T_o is 2000 K. The value of Q_{ext} decreases asymptotically as G increases because of the increase in the heat flux at the gas-solid interface. In other words high values of stagnation-point heat flux elevate the stagnation-point temperature, and, hence, enhance the chemical reactions that lead to the onset of ignition. A comparison shows that for the same operating conditions NC absorbs the least amount of heat before ignition takes place. This is consistent with the fact the reaction mechanism steps corresponding to NC have lower activation energies than the ones corresponding to the other solid materials. The comparison also shows that in order to get TATB to ignite it demands more heat addition than the other materials under consideration. This is explained by two factors. First, the values of the activation energy corresponding to TATB's reaction mechanism are higher than those corresponding to the other materials, and second, TATB has the highest thermal conductivity among all other solid materials, which enhances the heat diffusion through the solid region, and consequently makes the solid material require more external heat addition to ignite.

The effect of the gas temperature at the jet exit T_o on the ignition process of the solid materials under consideration is of great importance to the present study. Figure 11 presents several curves that describe the stagnation-point temperature histories for HMX-He with $G = 4.0 \times 10^7$ m^{-2}. Each curve corresponds to a different value of T_o. As shown in Fig. 11, T_o takes the values 1600, 1800, 2000, 2200, 2400, 2600, 2800, and 3000 K. For each value of T_o, the stagnation-point temperature increases with time until it reaches the thermal run-away condition that resembles the onset of ignition. The observation can be made that the ignition delay decreases as T_o increases because of the increase of the heat flux at the gas-solid

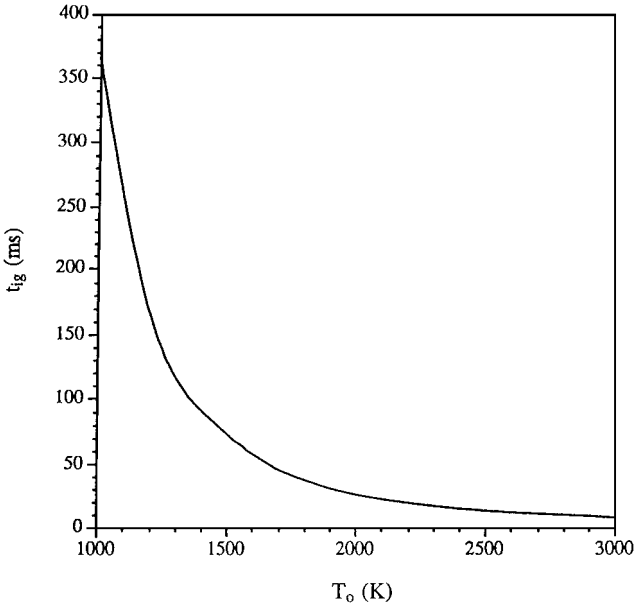

Fig. 12 Effect of T_o on the ignition delay t_{ig} for HMX-He with $G = 4.0 \times 10^7$ m^{-2}.

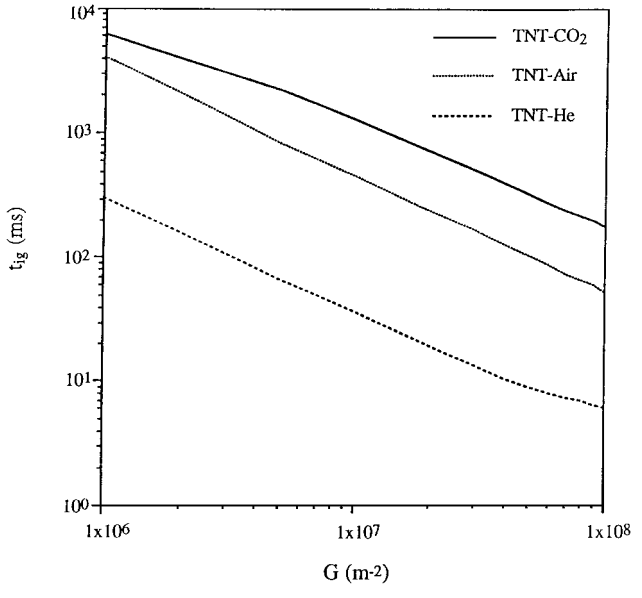

Fig. 13 Variation of the ignition delay t_{ig} with G for TNT-CO_2, TNT-Air, and TNT-He with T_o = 2000 K.

interface associated with the increase in T_o. For a given value of G, the ignition delay t_{ig} decreases asymptotically as T_o increases. This behavior is shown in Fig. 12 for HMX-He with $G = 4.0 \times 10^7$ m^{-2}. The variation of the ignition delay with T_o is explained by the strong correlation between T_o and the heat flux at the gas-solid interface.

The effect of the thermal properties of the impinging gases on the ignition process was studied in Fig. 13. The figure shows the variation of t_{ig} with G on the impingement of three different gases against TNT. These gases are carbon dioxide, air, and helium. Comparing the three cases corresponding to the impingement by carbon dioxide, air, and helium, the study showed that TNT had the shortest ignition delay when helium was used, whereas carbon dioxide yielded the longest ignition delay for the same values of G. This is because the thermal diffusivity of helium is the highest, whereas that of carbon dioxide is the lowest among the three gases investigated, and, hence, for a given temperature helium delivers the most amount of heat, whereas carbon dioxide delivers the least amount of heat to the solid material.

Conclusions

A mathematical model was developed to simulate the ignition of a reactive solid energetic material by a hot-gas impingement. The simulation involved a coupling of several phyisico-chemical processes that take place before the onset of ignition including the transfer of momentum within the fluid region and the conjugate heat-transfer characteristics of both the fluid and the solid regions. The model was applied to several energetic materials including HMX, RDX, TNT, TATB, and NC. Also, different types of impinging gases were investigated such as air, carbon dioxide, and helium. The predicted behavior of the condensed-phase temperature profiles suggest that the inert heating approach is not appropriate to simulate the ignition of the materials under consideration because it does not take into account the effect of the endothermic reactions that can precede the onset of ignition.

For the gas-solid combinations under investigation, and over the range of operating conditions of a hydrodynamic quantity G between 1×10^6 and 1×10^8 m^{-2}, and a jet-exit temperature T_o between 1000 and 3000 K, results of the present work show that the one-dimensional (axial) analysis has good agreement with the two-dimensional (radial and axial) calculations. Thus, the conclusion was made that the one-dimensional analysis could successfully reproduce the results of the two-dimensional analysis in regard to ignition characteristics. However, this statement may not be generalized for any operating conditions.

The hydrodynamic characteristics of the impinging gases have great influence on the ignition process of the solid materials. The observation can be made that the ignition delay decreases as G increases because of the increase in the heat flux at the gas-solid interface associated with the increase in G. For a given jet-exit temperature the ignition delay decreases asymptotically as G increases. The present study shows that for the same operating conditions NC has the shortest ignition delay, whereas TATB takes the longest time to ignite compared to the rest of the solid materials under consideration. The ignition characteristics of the solid energetic materials are determined by several factors including 1) the heat flux history at the gas-solid interface, 2) the heat loss to the environment, 3) the chemical kinetic characteristics of the chemical reactions within the solid material of interest, and 4) the physical properties of the solid materials. Although the heat flux appears to reach its steady-state value in a relatively short period of time, steady-state analysis cannot capture the thermal transients of the system accurately at early times and during the pyrolysis endothermic reactions, especially when G is less than 4.0×10^7 m^{-2}.

One other parameter of interest is the total amount of heat absorbed by the solid material before ignition takes place Q_{ext}. The value of Q_{ext} decreases asymptotically as the heat flux at the gas-solid interface increases. Results show that under the same operating conditions NC absorbs the least amount of heat before ignition takes place, whereas to get TATB to ignite, it demands more heat addition than the other materials under consideration. The gas temperature at the jet exit has a major effect on the ignition process. For given value of G, the ignition delay decreases asymptotically as the jet-exit temperature increases. The variation of the ignition delay with T_o is explained by the strong positive correlation between T_o and the heat flux at the gas-solid interface.

References

[1] Hobbs, M. L., Baer, M. R., and Gross, R. J., "Modeling Ignition Chemistry," JANNAF Systems Hazards Meeting, May 1993.

[2] Kulkarni, A. K., Kumar, M., and Kuo, K. K., "Review of Solid Propellant Ignition Studies," *Proceedings of the AIAA/SAE/ASME 16th Joint Propulsion Conference*, 1980.

[3] Kovalskii, A. A., Khlevnoi, S. S., and Mikheev, V. F., "The Ignition of Ballistite Powders," *Combustion, Explosion, and Shock Waves*, Vol. 3, 1967, pp. 527–541.

[4] Baer, A. D., and Ryan, N. W., "An Approximate but Complete Model for the Ignition Response of Solid Propellants," *AIAA Journal*, Vol. 6, 1968, pp. 872–877.

[5] Baer, A. D., and Ryan, N. W., "Evaluation of Thermal-Ignition Models from Hot-Wire Ignition Tests," *Combustion and Flame*, Vol. 15, 1970, pp. 9–21.

[6]Andersen, W. H., "Theory of Surface Ignition with Application to Cellulose, Explosives and Propellants," *Combustion Science and Technology*, Vol. 2, 1970, pp. 213–221.

[7]Thompson, C. L., Jr., and Suh, N. P., "The Interaction of Thermal Radiation and M2 Double-Base Solid Propellant," *Combustion Science and Technology*, Vol. 2, 1970, pp. 59–66.

[8]Bradley, H. H., Jr., "Theory of Ignition of a Reactive Solid by Constant Energy Flux," *Combustion Science and Technology*, Vol. 2, 1970, pp. 11–20.

[9]Linan, A., and Williams, F. A., "Theory of Ignition of a Reactive Solid by a Constant Energy Flux," *Combustion Science and Technology*, Vol. 3, 1971, pp. 91–98.

[10]Linan, A., and Williams, F. A., "Radiant Ignition of a Reactive Solid with In-Depth Absorption," *Combustion and Flame*, Vol. 18, 1972, pp. 85–97.

[11]Kindelan, M., and Williams, F. A., "Theory for Endothermic Gasification of a Solid by Constant Energy Flux," *Combustion Science and Technology*, Vol. 10, 1975, pp. 1–19.

[12]Bush, W. B., and Williams, F. A., "Influence of Strong Conductive Gas-Phase Cooling on Radiant Ignition of a Reactive Solid," *Combustion and Flame*, Vol. 27, 1976, pp. 321–329.

[13]Niioka, T., and Williams, F. A., "Ignition of a Reactive Solid in a Stagnation-Point Flow," *Combustion and Flame*, Vol. 29, 1977, pp. 43–54.

[14]Zumbrunen, D. A., "Convective Heat and Mass Transfer in the Stagnation Region of Laminar Jet Impinging on a Moving Surface," *Journal of Heat Transfer*, Vol. 113, 1991, pp. 563–570.

[15]White, F. M., *Viscous Fluid Flow*, McGraw–Hill, New York, 1974.

[16]Yao, L. S., and Prusa, J., "Melting and Freezing," *Advances in Heat Transfer*, Vol. 19, edited by J. P. Harnett and T. F. Irvine, Academic Press, New York, 1989.

[17]Gross, R. J., Baer, M. R., and Hobbs, M. L., "A Heat Transfer/Chemical Kinetics Computer Program for Multilayered Reactive Materials," Sandia National Lab., Energetic Materials and Fluid Mechanics Dept., SAND93-1603, Albuquerque, NM, 1993.

[18]Smith, T. F., Shen, Z. F., and Friedman, J. N., "Evaluation of Coefficients for the Weighted Sum of Gray Gases Model," *Journal of Heat Transfer*, Vol. 104, 1982, pp. 602–608.

[19]McGuire, R. R., and Tarver, C. M., "Chemical Decomposition Models for the Thermal Explosion of Confined HMX, TATB, RDX, and TNT Explosives," *Seventh Symposium (International) of Detonation*, Naval Surface Weapons Center, MP 82-334, 56, 1981.

[20]Schiesser, W. E., *The Numerical Method of Lines*, Academic International Press, San Diego, CA, 1991.

[21]Hindmarsh, A. C., LSODE (integration package), Mathematics and Statistics Sec., L-300, Lawrence Livermore Lab., Livermore, CA, 1980.

[22]Alkam, M. K., "Ignition of Solid Energetic Materials by Hot Gas Impingement," Ph.D Dissertation, Dept. of Mechanical Engineering, Univ. of Iowa, Iowa City, IA, Dec. 1995.

[23]Alkam, M. K., and Butler, P. B., "Transient Conjugate Heat Transfer Between a Laminar Stagnation Zone and a Solid Disk," *Journal of Thermophysics and Heat Transfer*, Vol. 8, No. 4, 1994, pp. 664–669.